Long-Term Ozone Exposure Attenuates 1-Nitronaphthalene–Induced Cytotoxicity in Nasal Mucosa

Myong Gyong Lee*,[1], Åsa M. Wheelock*,[2,3], Bridget Boland[2], and Charles G. Plopper[1]

Departments of [1]Anatomy, Physiology, and Cell Biology, and [2]Molecular Biosciences, School of Veterinary Medicine, University of California, Davis, California; and [3]Division of Respiratory Medicine, Department of Medicine, Karolinska Institutet, Stockholm, Sweden

1-Nitronaphthalene (1-NN) and ozone are cytotoxic air pollutants commonly found as components of photochemical smog. The mechanism of toxicity for 1-NN involves bioactivation by cytochrome P450s and subsequent adduction to proteins. Previous studies have shown that 1-NN toxicity in the lung is considerably higher in rats after long-term exposure to ozone compared with the corresponding filtered air–exposed control rats. The aim of the present study was to establish whether long-term exposure to ozone alters the susceptibility of nasal mucosa to the bioactivated toxicant, 1-NN. Adult male Sprague-Dawley rats were exposed to filtered air or 0.8 ppm ozone for 8 hours per day for 90 days, followed by a single treatment with 0, 12.5, or 50.0 mg/kg 1-NN by intraperitoneal injection. The results of the histopathologic analyses show that the nasal mucosa of rats is a target of systemic 1-NN, and that long-term ozone exposure markedly lessens the severity of injury, as well as the protein adduct formation by reactive 1-NN metabolites. The antagonistic effects were primarily seen in the nasal transitional epithelium, which corresponds to the main site of histologic changes attributed to ozone exposure (goblet cell metaplasia and hyperplasia). Long-term ozone exposure did not appear to alter susceptibility to 1-NN injury in other nasal regions. This study shows that long-term ozone exposure has a protective effect on the susceptibility of nasal transitional epithelium to subsequent 1-NN, a result that clearly contrasts with the synergistic toxicological effect observed in pulmonary airway epithelium in response to the same exposure regimen.

Keywords: goblet cell metaplasia; nasal transitional epithelium; 1-nitronaphthalene; ozone; protein adduct formation

1-Nitronaphthalene (1-NN) and close structural congeners are ubiquitous air pollutants primarily generated during combustion processes (e.g., diesel engine exhaust and wood smoke) and atmospheric photochemical reactions (1). In rat, the lung and liver are the major target organs of 1-NN cytotoxicity (2). Previous studies have suggested extensive involvement of cytochrome P450 monooxygenases (P450s or CYPs) in both hepatic and extrahepatic 1-NN bioactivation, with selective cytotoxicity of cell types containing high levels of P450s both in lung (Clara cells) and liver (hepatocytes) (2–4).

Increased rates of formation of 1-NN from naphthalene have been observed as the concentration of ozone increases (1). Once irradiated with ultraviolet rays ($\lambda < 320$ nm), molecular oxygen generates hydroxyl radicals, which efficiently initiates both ozone formation and nitration of ambient, volatile organic compounds such as naphthalene in the presence of NO/NO_2. The resulting co-exposure to ozone and 1-NN during photochemical smog episodes has raised the issue as to whether the impact of exposure to both toxicants would lead to an antagonistic or synergistic outcome. Previous studies looking specifically at lung tissue have demonstrated site-selective synergistic toxicological effects between the co-pollutants ozone and 1-NN. Interestingly, the susceptibility to 1-NN toxicity is significantly enhanced in the distal bronchioles of rat lung after long-term exposure to ozone compared with the corresponding lung injury seen in filtered air–exposed control rats (5). We have recently identified *in vivo* protein targets in lung for reactive 1-NN metabolites that are potentially associated with the mechanism of 1-NN toxicity and the synergistic effects of ozone in lung tissues (6).

Nasal mucosa from a range of mammalian laboratory species, including rats, mice, rabbits, and monkeys, is considered a "metabolic hot spot," with contents of P450s approaching hepatic levels in some cell types (7–9). Human nasal mucosa also shows P450 expression and activity (10–14), implying that nasal mucosa may be a major site of *in situ* 1-NN metabolism and toxicity also in humans (15). Activities of CYP2B1, reportedly the main isoform responsible for 1-NN activation (16), have been shown to be 20% higher in rat nasal mucosa than in lung parenchyma, and 2-fold higher than in liver (15). Consequently, a recent study showed that rat nasal mucosa sustains injury after 1-NN exposure. In the current study, we tested the hypothesis that the enhanced susceptibility to the bioactivated cytotoxicants 1-NN seen in the rat airway epithelium after long-term exposure to ozone extends also to the rat nasal passage.

Ozone-induced morphologic changes in nasal mucosa are well established in both rats and monkeys (17–20). These two species exhibit similar morphologic changes after short-term and long-term exposures. However, monkeys show a lower threshold than rats for ozone-induced changes. Conspicuously, changes induced by long-term ozone exposure in the rat nasal passage occur in a cell type–specific manner primarily in the nasal transitional epithelium (NTE). A marked initial neutrophil influx into the rat nasal transitional epithelium occurs after ozone exposure (21). Likewise, analysis of nasal lavage from human subjects exposed to ozone (0.4 ppm for 2 h) shows that ozone induces a significant influx of neutrophils in the upper respiratory tract also in humans (22). As ozone exposure continues in rat, neutrophil density decreases almost to baseline levels with concurrent development of goblet cell (mucin-containing epithelial cell) metaplasia and hyperplasia. The tolerance to further ozone exposure seen in the lower respiratory tract after 90 days of ozone exposure has not been reported in nasal mucosa (18), and the neutrophil-induced goblet cell metaplasia persists. In healthy adult humans, approximately 40% of inhaled ozone is absorbed in the nasal passages (23).

(*Received in original form November 8, 2005 and in final form September 11, 2007*)

*These two authors contributed equally to this manuscript.

This work was supported by National Institute of Environmental Health Sciences Grants ES00628, ES04311, and ES04699. The University of California Davis was an NIEHS Center for Environmental Health Sciences (ES05707), and support for core facilities used in this work is gratefully acknowledged. Å.M.W. was supported by University of California Toxic Substances Research and Teaching Program, and by EU Fp6 Marie Curie Fellowship 041417.

Correspondence and requests for reprints should be addressed to Åsa M. Wheelock, PhD, Lung Research Lab L4:01, Respiratory Medicine Unit, Department of Medicine, Karolinska Institutet, 171 76 Stockholm, Sweden. E-mail: asa@para-docs.org

Am J Respir Cell Mol Biol Vol 38. pp 300–309, 2008
Originally Published in Press as DOI: 10.1165/rcmb.2005-0416OC on September 27, 2007
Internet address: www.atsjournals.org

In parallel to our previous lung studies, the current study aimed to examine the impact of exposure to ozone and 1-NN on the integrity of nasal mucosa, as well as the protein binding of reactive 1-NN metabolites in the various mucosal epithelia present in the nasal passage.

MATERIALS AND METHODS

Chemicals

The following chemicals were used: Alcian blue (J. T. Baker, Phillipsburg, NJ), formic acid (Merck KgaA, Darmstadt, Germany), glacial acetic acid (Fisher Scientific, Fair Lawn, NJ), glycol methacrylate resin (Electron Microscopy Sciences, Fort Washington, PA), paraformaldehyde and sodium meta-bisulfite (Fisher Scientific, Gibbstown, NJ), periodic acid (Fisher Scientific), Schiff's reagent (Sigma-Aldrich, St. Louis, MO), and toluidine blue (Polysciences, Warrington, PA). Ultrapure urea was obtained from U.S. Biological Corp (Cleveland, OH). Omnipure TRIS, glycine, and SDS were purchased from EM Sciences (Gibbstown, NJ). CHAPS, Protease inhibitor cocktail III, and Triton X-100 were acquired from Calbiochem (La Jolla, CA). Bradford protein assay reagent and PVDF Sequi-blot membranes were obtained from Bio-Rad (Hercules, CA). Bovine serum albumin (BSA), thiourea, and dithiothreitol (DTT) were ordered from Sigma-Aldrich. IsoGel low EEO agarose was ordered from BMA (Rockland, ME), ^{14}C-1-NN was synthesized as previously described (13). Rhinohide was purchased from Molecular Probes (Eugene, OR). All other electrophoresis materials and equipment were obtained from Amersham Biosciences (Piscataway, NJ). All solutions were prepared with deionized water (resistivity 18.1 MΩ/cm).

Animals

Male Sprague-Dawley rats were purchased from Harlan Laboratories (San Diego, CA). Animals were provided with food and water *ad libitum* and were housed in an AAALAC-accredited facility in HEPA-filtered cage racks at the University of California, Davis, for at least 7 days before use in an experiment.

Treatment

Forty-eight rats (68–71 d old) were divided into 14 exposure groups, and exposed to ozone and/or 1-NN as outlined in Table 1. Initially, the rats were exposed to filtered air (FA) or 0.8 ppm ozone (O_3) for 8 hours per day (midnight to 8:00 A.M.), daily for 90 days as previously described (5). The dose regimen was intentionally set to approximately 4-fold higher than typical peak values in polluted urban areas, since the rat respiratory system has been shown to be much less sensitive to ozone than that of nonhuman primates. As such, exposures to concentrations greater than 0.5 ppm are required to mimic the pathologic effects on the primate lung at ambient ozone concentrations (24). The rats were removed from ozone exposure for at least 24 hours before 1-NN exposure. On the 91st day, the rats (462.9 ± 25.6 g of body weight) were treated with 0, 12.5, or 50.0 mg of 1-NN/kg of body weight in corn oil (CO) (Mazola, Cordova, TN) by intraperitoneal injection (n = 4). The two groups used for quantification of adduct formation in the nasal epithelium received 50.0 mg/kg of ^{14}C-labeled 1-NN (specific activity 2,214 dpm/nmol, n = 5). All injections were performed between 8:00 A.M. and 12:00 noon. Rats were anesthetized with a lethal dose of sodium pentobarbital 2, 6, or 24 hours after 1-NN intraperitoneal injections (*see* Table 1), and nasal tissue was isolated as described below.

TABLE 1. NUMBER OF ANIMALS EXPOSED TO O_3 (0.8 ppm, 8 h/d, DAILY FOR 90 d) AND 1-NN (INTRAPERITONALLY)

	FA	O_3	FA	O_3	FA	O_3
Time after 1-NN Treatment	2 h		6 h		24 h	
0 mg of 1-NN/kg			4	4	4	4
12.5 mg of 1-NN/kg			4	3	4	4
50 mg of 1-NN/kg	5*	5*	4	4	4	4

Definition of abbreviations: 1-NN, 1-nitronaphthalene; FA, filtered air.
* ^{14}C-labelled 1-NN.

Sample Preparation for High-Resolution Histopathology

After anesthetization, the animals were exsanguinated by cutting the abdominal aorta. After the lower jaw was removed, the head was separated from the cadaver. The nasal passage was flushed with 6 ml of ice-cold 4% paraformaldehyde (0.1 M sodium phosphate buffer, pH 7.4) through the nasopharyngeal duct. Then the nasal passage was placed in 60 ml of ice-cold 4% paraformaldehyde and briefly placed under vacuum, and then fixed at 4°C for at least 24 hours. The fixed nasal passage was decalcified in 60 ml of 13% formic acid with gentle shaking for 5 days at room temperature. The decalcified nasal passage was washed with running tap water for 4 hours to remove formic acid from the specimen and was grossly sectioned perpendicular both to the mouth palate and to the nasal septum at the following four specific anatomic locations (25): (*1*) (block 1) immediately posterior to the upper incisive teeth, (*2*) (block 2) through the incisive papilla, (*3*) (block 3) through the second palatal ridge, and (*4*) (block 4) in the middle of the first upper molar teeth. The sections were embedded in glycol methacrylate. Four-micron sections were cut from each embedded section using a Zeiss Microm HM340E microtome (Carl Zeiss, Thornwood, NY). Sections were stained with 1% toluidine blue for examination by high-resolution light microscopy.

Quantitative Histopathology

Histopathologic changes were quantified by stereologic approaches (26) using a cycloid grid overlay and software for counting points and intercepts (Stereology Toolbox, Davis, CA). The volume fraction of epithelial cells, intraepithelial mucosubstances, or vacuoles (closed empty space within the epithelial layer) was calculated respectively through the formula $V_v = P_n/P_r$, where P_n is the number of points hitting the object of interest, and P_r is the number of points hitting the reference space, the epithelium. To assess the degree of hyperplasia induced by long-term ozone exposure, the number of points hitting the nuclei of epithelial cells were divided by the number of intercepts crossing the basement membrane and compared among treatment groups. The height (τ) of the epithelium was obtained by the following formula: $\tau = V_v/S_v$, where V_v indicated the sum of the volume fraction of epithelial cells, intraepithelial mucosubstances, and vacuoles per reference space. S_v was defined by the surface area of the basement membrane per reference space: $S_v = 2\ I_o/L_r$, where I_o is the number of intercepts with the basement membrane, and L_r is the length of test line in the reference space. The volume of a mixed population of inflammatory cells present in the lamina propria, outside the blood vessel, per surface area of the basement membrane, was obtained to compare the degree of infiltration of inflammatory cells between the treatment groups.

Histochemistry by Alcian Blue–Periodic Acid-Schiff at pH 2.5

Acidic glycoproteins are Alcian blue (AB)-positive and stain blue, while neutral glycoproteins are periodic acid-Schiff (PAS)-positive and stain bright pink to magenta. Four-micron serial, glycol methacrylate sections were stained with AB-PAS, AB, or PAS using the same batch of staining solutions according to standardized methods for paraffin sections, except that the sections were incubated with each dye at a higher temperature (60°C).

Determination of Total ^{14}C-1-NN Protein Binding

Transitional epithelium (from maxilloturbinates), respiratory epithelium (from nonolfactory septal epithelium), and olfactory epithelium (from septum) was isolated through microdissection from rats exposed to ^{14}C-labeled 1-NN (Table 1). Samples were homogenized in lysis buffer (2 M thiourea, 7 M urea, 4% wt/vol CHAPS, 0.5% wt/vol Triton X-100, 1% wt/vol [65 mM] DTT, and 2% vol/vol protease inhibitor cocktail III) as previously described (6). Acetone precipitation was performed on four of the five samples from each exposure group through the addition of 2 volumes of ice-cold acetone followed by centrifugation at 4,000 × g for 10 minutes at room temperature. The supernatant was discarded, and the pellet resuspended in acetone. The procedure was repeated until the radioactivity of the supernatant did not exceed background levels. The pellet was then resuspended in 2 N NaOH, the protein concentration was determined with the method of Bradford (27), and the radioactivity was measured in duplicate through

scintillation count. The first four supernatants were collected, evaporated to dryness, and reconstituted for protein concentration determination. No leakage of protein into the supernatant occurred. Due to the low amounts of protein recovered from some of the samples, scintillation counts of less than 100 DPM were deemed too have too low signal-to-noise ratio and were excluded from further analysis. A minimum of three samples from each group were used in statistical analyses.

The three different tissues from the fifth sample of each exposure group were separated on individual 18-cm immobilized pII gradient (IPG) strips (pH 4–7) using all isolated protein (262–468 μg protein). IPG buffer was added to a final concentration of 1% vol/vol, and samples were diluted to 350 μl with lysis buffer. The protein sample was loaded onto the IPG strip through rehydration at room temperature overnight, and isoelectric focusing (IEF) was performed using a Multiphor II Electrophoresis unit at 20°C for a total of 74.9 kVh. IPG strips were incubated 2 × 15 minutes in equilibration buffer (50 mM tris-HCl pH 8.8, 6 M urea, 30% glycerol, 2% SDS). Reduction and alkylation of sulfhydryls was performed through incorporation of 65 mM DTT in the first incubation, and 10 mM iodoacetamide in the second. The strips were sealed using 0.5% IsoGel agarose. The second dimension was performed on 10%T Rhinohide acrylamide gels in a Hoefer ISO- DALT 2D Electrophoresis system at 10°C, 14 mA/gel until the dye front had migrated 17 cm (~ 18 h) in 25 mM Tris, 192 mM glycine, and 0.1% SDS. After electrophoresis, the protein gels were electroblotted to Sequi-blot PVDF membranes (0.2μm pore size) at 10°C, 250 mA for 19 hours in 25 mM Tris, 192 mM glycine, 10% (vol/vol) methanol. The membranes were then washed with water (3 × 30 min) followed by 30 minutes in 60% methanol and dried in a vacuum desiccator before protein visualization.

Phosphorimaging

Low-energy Storage Phosphorimaging Screens (Fuji, Stamford, CT) were exposed to PVDF membranes for 67 days. The plates were simultaneously exposed to protein standards created through dot-blotting a dilution series of ^{14}C-BSA (Sigma-Aldrich) to a strip of PVDF membrane. The ^{14}C-BSA was diluted with cold BSA, and the protein content in each dot-blot was kept constant. The radioactive protein spots were visualized using a Typhoon laser scanner and quantified using Image Quant software and a standard curve from the ^{14}C-BSA standard strip. The limit of detection was 0.0064 DPM, which is equivalent to 3 fmol adducted 1-NN.

Statistical Analyses

All pathology data were expressed as mean ± 1 SD. Four to six fields per each animal were captured for stereological analysis. All data were imported into Prism 4.02 (GraphPad, San Diego, CA) for statistical analysis. Differences between treatment groups were determined by one-way ANOVA. Significance was determined at the 95% confidence level. For protein binding data, mean and standard deviation values were calculated on all data sets, and two-tailed, paired, *t* tests were performed using Microsoft Excel.

RESULTS

Due to the systemic route of exposure used for the bioactivated toxicant, this study is examining target cell type selectivity rather than the site selectivity of the toxicant. Taken together, the anterior faces of blocks 1 (T1) and 3 (T3) reflect the major epithelial cell populations present in nasal tissues. Accordingly, the pathologic effects observed in these locations are reported in the result section below. Histologic changes due to 1-NN exposure were observed only in the groups treated with 50 mg/kg. Unless stated, the degree of injury from 50 mg of 1-NN/kg was similar between 6 and 24 hours after treatment, and data presented here are those from 6 hours after treatment.

High-Resolution Histopathology of the NTE at the Anterior Portion of the Nasal Passage (T1)

In rats exposed to filtered air and corn oil vehicle (FA+CO), NTE was the predominant epithelial population in the anterior portion of the nasal passage (T1). NTE was not found in the posterior portion (T3) of the nasal passage. At T1, NTE lines the maxilloturbinates, part of the nasoturbinates, and the lateral wall of the lateral meatus (Figure 1A, NTE marked in *yellow*). Furthermore, the presence of goblet cells was confined to the respiratory epithelium lining the nasal septum in T1 sections (Figure 1A, respiratory epithelium marked in *blue*).

In accordance with previous reports (18), the NTE in the FA+CO-exposed rats was one to two cells thick and composed mostly of nonciliated, cuboidal/columnar cells (Figure 1B). The height of the NTE of the FA+CO rats was 9.9 ± 2.4 μm (Figure 2A). The epithelium was free of intraepithelial vacuoles (Figure 2D) and of inflammatory cell infiltrates (Figure 2E).

After 1-NN exposure, the NTE of the FA-exposed rats sustained severe inflammation and injury (Figure 1C). Basal cells seemed unaffected by 1-NN treatment, and the majority remained attached to the basement membrane. In the underlying lamina propria, the blood vessels of FA+1-NN–exposed rats were dilated. Furthermore, the acellular matrix in the underlying lamina propria of NTE was substantially edematous and was abundant in inflammatory cells, predominantly polymorphonuclear cells (Figures 1B versus 1C).

Even though injury from 1-NN was severe in the NTE, the height of the epithelial layer in the FA+1-NN rats (14.17 ± 4.3 μm) was not significantly different from the FA+CO control rats (Figure 2A). This is attributed to intraepithelial vacuole formation (35.1 ± 9.7% of the epithelium by volume) (Figure 2D) and cytoplasmic swelling in the NTE of the FA+1-NN rats. Both intracellular and extracellular vacuolarization was observed, the latter being an intracytoplasmic sign of early injury. This injury seen in high-resolution histopathology such as methacrylate sections generally do not lose membrane integrity, and proves to be reversible (28, 29). The number of intraepithelial nuclei in the FA+1-NN rats was not significantly different compared with FA+CO control rats. Intraepithelial vacuole formation and inflammatory cell infiltrates in the FA+1-NN rats were the highest among all treatment groups (Figures 2D and 2E).

Long-term ozone exposure elicited a chronic lesion similar to what previously has been reported for rat nasal mucosa (18), and marked goblet cell metaplasia in the NTE region (Figure 1D) was observed in rats exposed to ozone and corn oil vehicle (O_3+CO), The metaplastic epithelium of the ozone-exposed rats was composed of goblet cells, nonciliated cuboidal/columnar cells, and basal cells. Atrophy of turbinate bone (labeled tb in Figure 1) was evident in the maxilloturbinates and nasoturbinates, which was not seen in the FA-exposed rats. The only sign of ozone-induced injury in the metaplastic epithelium was a low density of inflammatory cells present in the underlying lamina propria.

The height of the metaplastic epithelium in the O_3+CO rats was 23.0 ± 1.7 μm, corresponding to a 133% increase ($P < 0.0001$, Figure 2A) compared with FA+CO-exposed controls (Figure 2A). The average volume of nuclei per unit basement membrane surface area increased by 72.6% ($P = 0.0062$) in the metaplastic epithelium of the O_3+CO rats compared with the FA+CO rats. The increased nuclear volume was the result of an increase in number in nuclei; the size of the nuclei remained the same, thus indicating an incidence of hyperplasia (Figure 2B). Intraepithelial mucosubstances were most prominent in the apex of the metaplastic goblet cells (49.1 ± 3.4% of the epithelium by volume; Figure 2C). Furthermore, only 0.2 ± 0.0% of the epithelium was occupied by intraepithelial vacuoles (Figure 2D). A low density of inflammatory cells was present in the underlying lamina propria of the metaplastic epithelium (Figure 2E).

Long-term exposure to ozone before 1-NN exposure (O_3+1-NN) resulted in an attenuation of the injury from 1-NN (Figure 1E). The lamina propria of the metaplastic epithelium of the

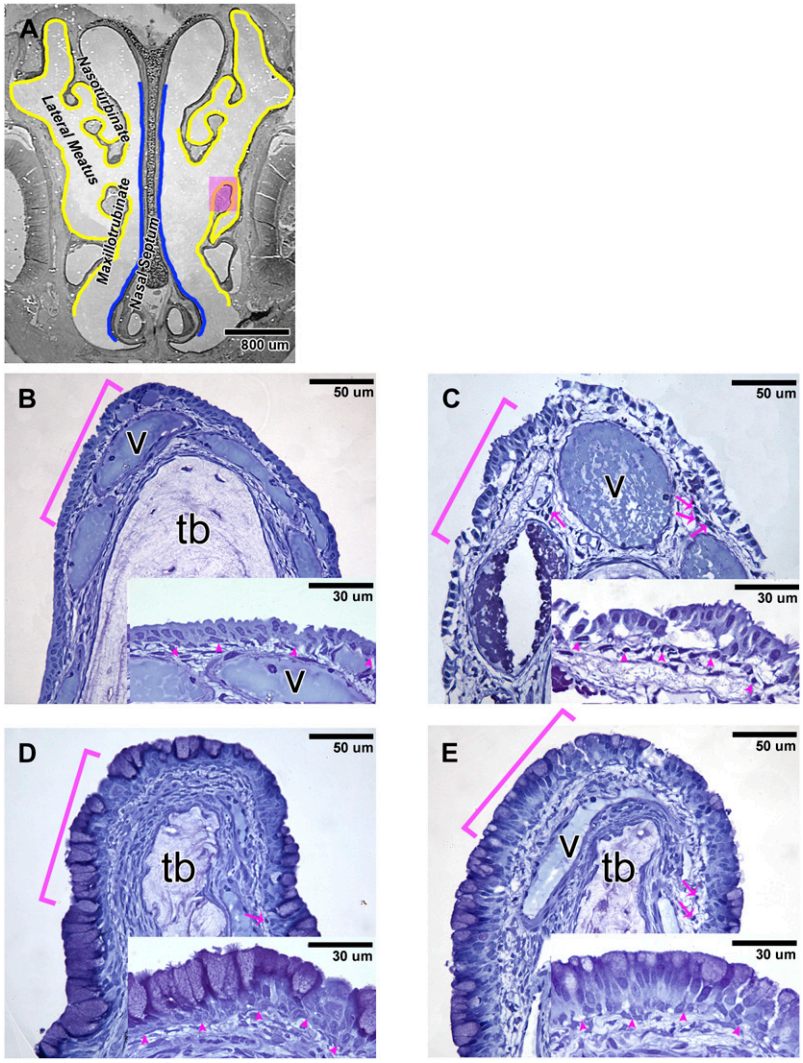

Figure 1. (*A*) Distribution of the nasal transitional epithelium (NTE) (marked in *yellow*) and respiratory epithelium (marked in *blue*) at the anterior portion of the nasal passage (T1) of rats exposed to filtered air (FA) + corn oil (CO). High-resolution histopathology of the NTE stained with toluidine blue from rats treated with (*B*) FA + CO, (*C*) FA+1-nitronaphthalene (1-NN), (*D*) O_3+CO, and (*E*) O_3+1-NN at 6 hours after CO/1-NN treatment. *B*, *C*, *D*, and *E* are high-magnification images of the *pink-shaded* maxilloturbinate on *A*. *Insets* are high-magnification images of the *bracketed areas*. In the O_3+CO rats, marked goblet cell metaplasia and mild hyperplasia occurred (*D*). The metaplastic epithelium of the O_3+1-NN rats (*E*) sustained much less 1-NN injury than that of the FA+1-NN rats (*C*). *Arrowheads*, basement membrane; *arrows*, polymorphonuclear cells; b, basal cells; g, goblet cells; n, nonciliated cuboidal/columnar cells; tb, turbinate bone; v, blood vessel.

O_3+1-NN rats appeared less edematous than the lamina propria of the NTE of the FA+1-NN rats (Figures 1E versus 1C). The epithelial height and the number of intraepithelial nuclei in the O_3+1-NN rats did not change significantly (Figures 2A and 2B) compared with the O_3+CO rats. Intraepithelial mucosubstances in the metaplastic epithelium of the O_3+1-NN rats were depleted significantly compared with the O_3+CO rats (Figure 2C). After 1-NN treatment, 8.6 ± 2.5% of the metaplastic epithelium by volume was occupied by vacuoles in the O_3+1-NN rats, which was significantly lower volume than in the NTE of FA+1-NN rats (38.0 ± 9.6%) (Figure 2D). In the lamina propria outside of the blood vessels, the average volume of inflammatory cells per unit area of basement membrane was approximately 2-fold less ($P = 0.0014$) in the metaplastic epithelium of O_3+1-NN exposed rats compared with the infiltration seen in the NTE of FA+1-NN exposed rats (Figure 2E).

High-Resolution Histopathology of the Anterior Portion of the Nasal Passage (T1) by AB-PAS (pH 2.5) Histochemistry

Examination of 4-μm serial sections stained with either AB-PAS, AB, or PAS demonstrated that the NTE in FA+CO-exposed control rats was AB-PAS–negative (Figure 3A). In contrast, the ozone-induced goblet cell metaplasia in O_3+CO-exposed rats resulted in a marked up-regulation of both AB-positive (Figure 3C) and PAS-positive (Figure 3D) mucosubstances. However, ozone exposure did not appear to alter the amount/composition of AB-PAS–positive materials in nonmetaplastic goblet cells that are present in respiratory epithelium (RE) of nasal septum (data not shown)

High-Resolution Histopathology of the Posterior Portion of the Nasal Passage (T3)

There were no differences in histology at the posterior portion of the nasal passage (T3) between FA+CO-exposed and O_3+CO-exposed rats. Moreover, long-term ozone exposure did not appear to alter susceptibility to 1-NN–induced injury in the nasal regions at T3 (data not shown). 1-NN injury in both FA-exposed and ozone-exposed rats occurred in all types of epithelia lacking goblet cells at T3, while epithelia containing goblet cells at T3 was not injured from 1-NN (data not shown). The incidence of olfactory mucosal injury from 1-NN was confined only to the area of the DMM (Figure 4B, injury at 6 h after 1-NN treatment shadowed in *red*). The area of olfactory mucosal injury from 1-NN became slightly broader at 24 hours than at 6 hours after 1-NN treatment, and the injury extended also to the small area (shaded in *blue* in Figure 4B) of the middle portion of the nasal septum at T3 (data not shown). In the olfactory epithelial layer, the continuity was disrupted, and the cytoplasmic volume of sustentacular cells was reduced due to 1-NN toxicity (Figure 4D). In the underlying lamina propria of injured olfactory epithelium, the toluidine blue staining of Bowman's glands appeared to be depleted by 1-NN treatment.

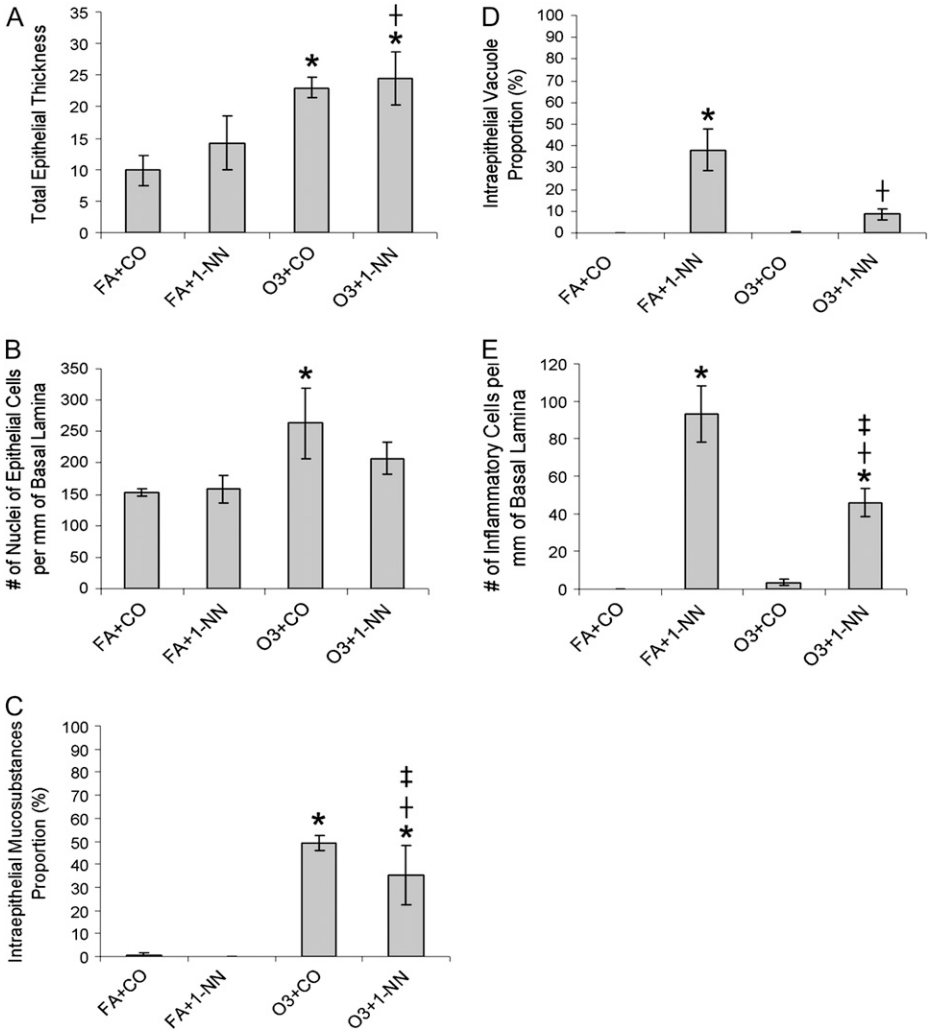

Figure 2. Quantitative histopathology of the NTE after treatment of rats with FA+CO, FA + 50 mg 1-NN/kg (FA+1-NN), ozone + CO (O_3+CO), or ozone + 50 mg 1-NN/kg (O_3+1-NN) at 6 hours after CO or 1-NN treatment. Data from 6- and 24-hour time points were not significantly different among the rats with the same treatment. *Significantly different from FA+CO; †O_3+1-NN is significantly different from FA+1-NN; ‡O_3+1-NN is significantly different from O_3+CO. Significance was determined at $P < 0.05$.

The adjacent olfactory sensory cells look intact. However, the nerve bundles in the lamina propria are no longer visible, which indicated that there were cytotoxic effects to the olfactory nerve bundles.

At T3, 1-NN injury in ciliated columnar epithelial cells in the main nasal passage (Figure 4F) as well as in the maxillary sinus (Figure 4H) was characterized by intraepithelial vacuole formation and inflammatory cell infiltrates. The diameter of blood

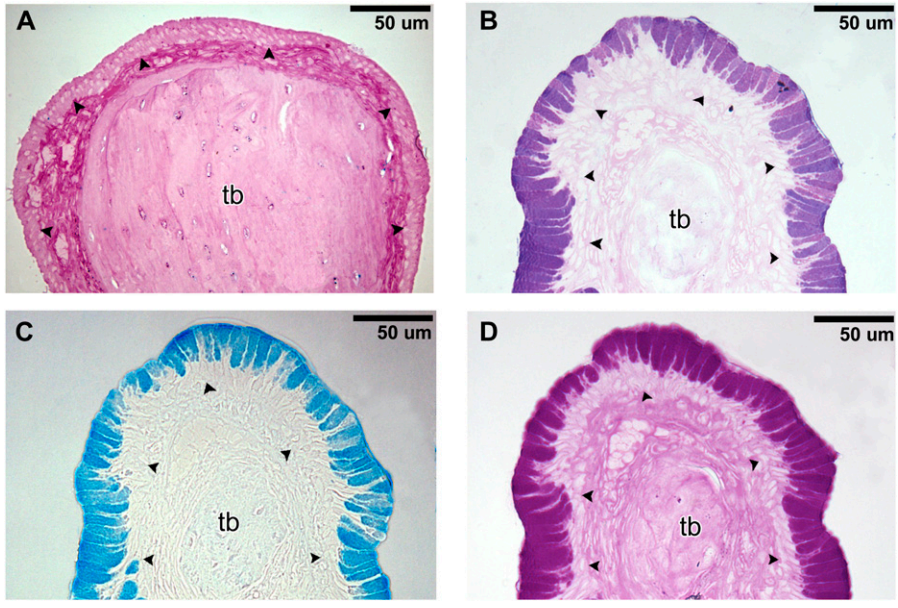

Figure 3. Histochemistry at the anterior portion of the nasal passage (T1) by Alcian blue-periodic acid-Schiff (AB-PAS) at pH 2.5 at 6 hours after CO treatment. (*A*) The maxilloturbinate stained with AB-PAS after FA+CO treatment. The maxilloturbinate stained with (*B*) AB-PAS, (*C*) AB, and (*D*) PAS after O_3+CO treatment. *Arrowheads*, basement membrane; tb, turbinate bone.

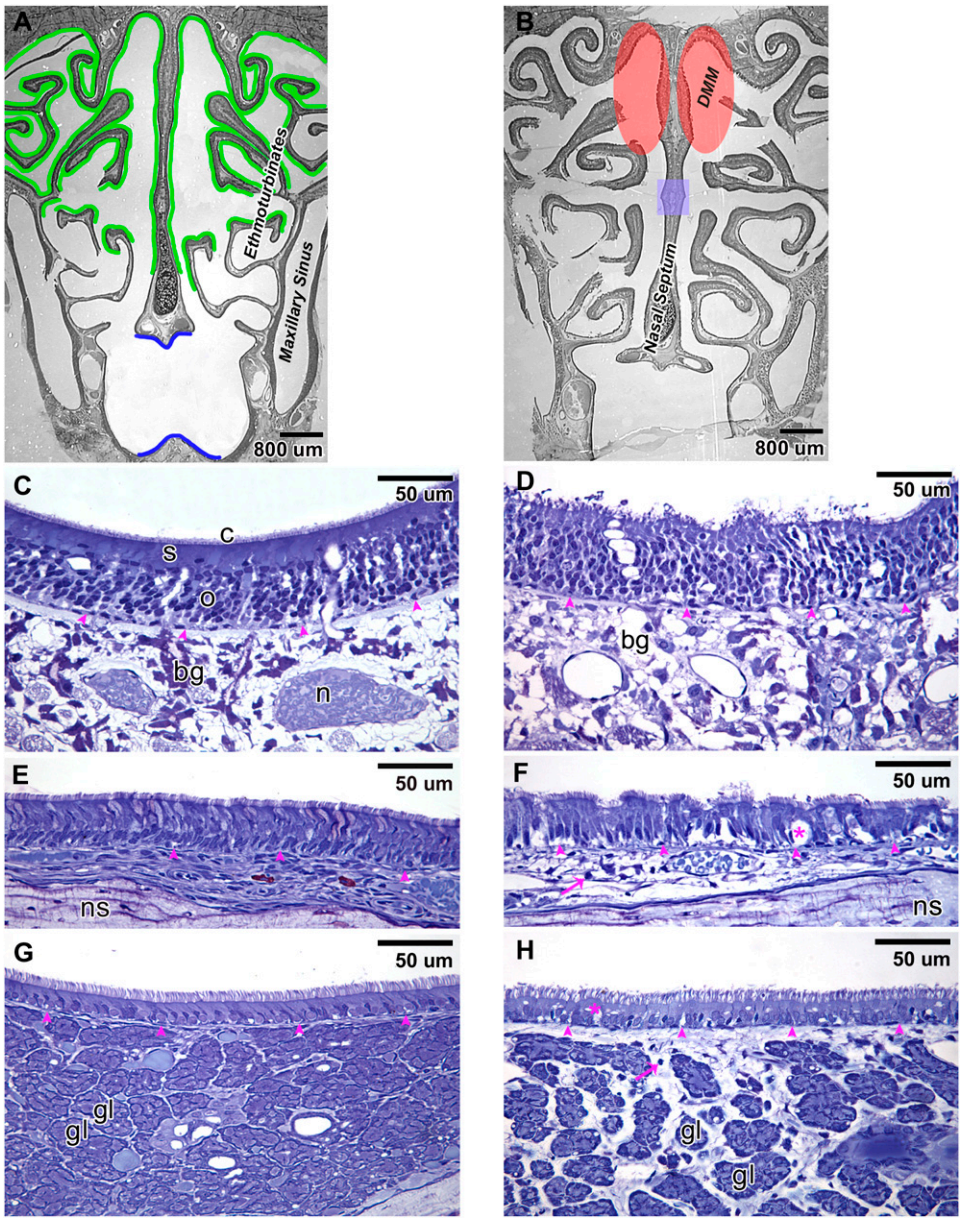

Figure 4. Distribution of the olfactory epithelium (marked in *green*) and the respiratory epithelium (marked in *blue*) at the posterior portion of the nasal passage (T3) of rats exposed to FA+CO (*A*). 1-NN injury was quite similar between the FA-exposed and O_3-exposed rats and occurred in all types of the epithelia that lack goblet cells at T3. The goblet cell–containing epithelium was not injured from 1-NN (data not shown). Olfactory mucosal injury from 1-NN was region-specific, unlike other types of epithelia, and it was confined only to the olfactory epithelium lining the dorsal medial meatus (DMM, shaded in *red*) at 6 hours after 1-NN treatment (*B*). At 24 hours after 1-NN treatment, the area of olfactory mucosal injury from 1-NN also included the small area (shaded in *blue*) of the middle portion of the nasal septum (*B*). High-resolution histopathology of the olfactory epithelium (*C* and *D*), the respiratory epithelium in the main nasal passage (*E* and *F*), and the respiratory epithelium in the maxillary sinus (*G* and *H*) is shown at 6 hours after CO (*C*, *E*, and *G*) or 1-NN (*D*, *F*, and *H*) treatment. *Arrowheads*, basement membrane; *arrows*, polymorphonuclear cells; bg, Bowman's glands; c, cilia from olfactory receptor cells; gl, gland; n, nerve bundle; ns, nasal septum; o, olfactory receptor cells; s, sustentacular cells; * vacuole.

vessels was significantly increased, and the acellular matrix was substantially swollen (Figures 4F and 4H). Secretory glands in the maxillary sinus that resided densely in the lamina propria were separated from each other due to the swelling of inflamed acellular matrix (Figure 4H).

1-NN Metabolite Binding

The overall 1-NN metabolite–protein binding determined through scintillation counting is displayed in Figure 5. The total protein adduction was significantly decreased ($\sim$ 2-fold) in ozone-treated animals (*solid bars*) compared with FA-exposed controls (*open bars*) in nonciliated respiratory epithelium, also termed NTE (Figure 5). No significant alteration in adduct formation was observed in olfactory epithelium (OE) or ciliated RE. Alterations in the adduction of specific protein species due to prior long-term ozone exposure were primarily observed in the NTE epithelium (Figure 6), but not in OE and RE. A total of 10 specific protein spots adducted by ^{14}C–1-NN metabolites were discernible on the storage phosphorimages. The location of six of these spots (Figure 6, *spots 1–6*) corresponded with proteins previously shown to be adducted both in target tissue (airway epithelium) and nontarget tissue (liver) (6). Furthermore, two of the spots (Figure 6, *spots 9* and *10*) were only adducted at detectable levels in NTE epithelium after long-term ozone exposure. Lastly, prior long-term ozone exposure appeared to drastically alter the adduction pattern of an additional protein in NTE (Figure 6, *spot 8*), with specific activities being 16-fold higher in the ozone-exposed animal compared with the control animal. Such dramatic differences in adduction levels between ozone-exposed and FA-exposed animals were not detected in OE and RE. Given that the analysis of specific protein adduction was performed on a single animal from each exposure group, the small differences in specific activities observed for the other proteins may be a result of inter-individual variation or technical variance.

DISCUSSION

In previous studies, we have shown that the bioactivated air pollutant 1-NN causes site- and cell type–selective lesions corresponding

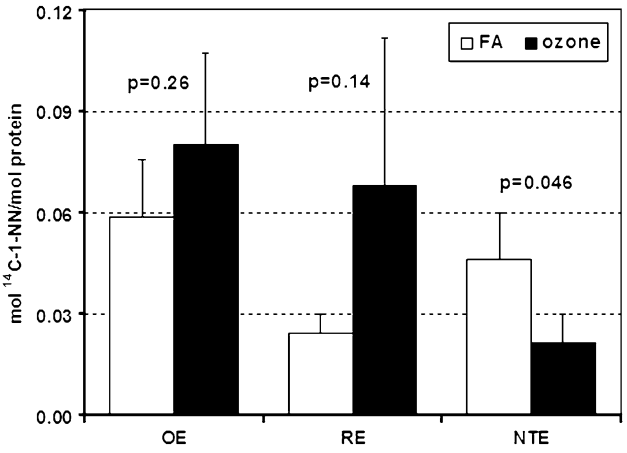

Figure 5. Total adduct formation by 1-NN metabolites in olfactory epithelium (OE), respiratory epithelium (RE), and NTE of FA-exposed animals (*open bars*) versus ozone-exposed animals (*solid bars*) 2 hours post injection of 50 mg/kg ^{14}C-1-NN. A statistically significant decrease in 1-NN metabolite binding was observed in the NTE of ozone-exposed animals compared with FA-treated control ($P = 0.046$). In contrast, no statistically significant alterations in metabolite binding were observed in RE ($P = 0.14$) or OE ($P = 0.26$). The values are expressed as mean ± SD ($n = 4$).

to the site of P450-mediated activation in the rat airway epithelium (30). Moreover, we have demonstrated that 1-NN–mediated cytotoxicity in the distal airways is synergized by prior long-term exposure to ozone (5, 31). In two companion studies, encompassing proteomics and metabolomics profiling of the airways of the same animals used in this study, we have shown that these synergistic effects may be related to an ozone-induced shift from a Th1-mediated to a Th2-mediated inflammatory response, leading to increased P450-mediated adduction of four specific proteins important in the cellular defense against oxidative stress as well as in regulation of the inflammatory response in the lung (6, 45). Nasal mucosal epithelium contains several cell types with high abundances of P450 enzymes, and as such is a potential metabolic hotspot for bioactivation of toxicants such as 1-NN. Recently, Foy and Schatz confirmed that 1-NN indeed induces lesions throughout the nasal mucosa, and that these lesions were attenuated by inhibition of P450 activity (15). In the current study, we investigated whether the synergistic effects of ozone and 1-NN seen in the lung extends also to the upper respiratory tract.

The results of this study indicate that injury and inflammation of nasal epithelium after systemic 1-NN treatment (50 mg/kg) was severe in adult male Sprague-Dawley rats. Injury to the olfactory epithelium caused by 1-NN occurred in a region-specific manner and appeared not to involve inflammatory cell infiltrate. In concurrence with previous studies, damage to the OE was primarily focused to the sustentacular cells, with mild damage to nerve bundles and Bowman's glands in the lamina propria (15), the latter manifested as a depletion of the toluidine blue staining of Bowman's glands (Figure 4D). This could be due to degenerative cellular changes in Bowman's gland or due to a secretion of intraepithelial mucosubstances in the mucous cells of these glands. A similar response has been observed after exposure to the mechanistically related cytotoxicant, naphthalene (32). OE has the highest levels of P450 s in nasal mucosa, primarily located to sustentacular cells and the to acinus area of Bowman's glands (9), and lesions to this epithelial type thus correspond well with the putative mechanism of toxicity.

In RE, 1-NN–induced lesions were characterized by vacuole formation and infiltration of inflammatory cells. The acute epithelial necrosis and exfoliation with inflammatory exudates reported by Foy and Schatz was not observed. However, these authors used a higher dose of 1-NN and a different route of administration (200 mg/kg per os [15]), which may account for the differing results. Similar effects of nonspecific lesions have been shown also in airways after exceedingly high doses (30). In polluted urban areas, we are exposed to low levels of 1-NN through inhalation of both the aerosol and particulates. Because no satisfactory regimen for inhalation exposure to 1-NN currently is available, the toxicant was administered through intraperitoneal injection in this study, as well as in the preceding pathology studies (5, 31). No studies correlating doses through different administration routes have been published for 1-NN. However, corresponding studies for the parent compound naphthalene, which has a similar mechanism of toxicity, correlated injury levels in distal airways after inhalation of current Occupational Safety and Health Administration standards (10 ppm) with intraperitoneal administration of 100 mg/kg in mice, approximately 25% of the median lethal dose (LD_{50}) (33, 34). In addition, we recently showed that 1-NN is activated in the airway epithelium before hepatic activation (also after intraperitoneal administration), and injury to the airway epithelium is likely independent of hepatic metabolism (6). Here, we used two doses: a low dose of 12.5 mg/kg, and a high dose of 50 mg/kg, approximately 36% of the LD_{50} (35) to match previous pathology studies.

In contrast to Foy and Schatz, we found that the NTE sustained the greatest epithelial injury after 1-NN administration, including intraepithelial vacuole formation, cytosolic swelling, and inflammatory cell infiltration in the lamina propria. Then again, no distinction between ciliated (RE) and nonciliated (NTE) respiratory epithelium was mentioned in the manuscript. Careful evaluation of the micrographs presented in conjunction with reports of the most prominent lesions occurring in the anterior portion of the nose implies that also the NTE may have been severely damaged after oral administration of 1-NN (15). More importantly, all 1-NN–related cytotoxicity was completely attenuated by prior m-xylene exposure (15), a well-documented inhibitor of the main P450 involved in 1-NN activation, CYP2B1 (15, 16).

In ozone-exposed rats, less severe injury (i.e., fewer inflammatory cell infiltrates and intraepithelial vacuoles) was observed after 1-NN exposure. This attenuation in toxicity occurred primarily in areas in which ozone caused goblet cell metaplasia and mild hyperplasia. Metaplastic and nonmetaplastic nasal goblet cells sustained very little 1-NN injury, which corresponds to the lack of toxic lesions from 1-NN seen in the goblet cells of the airway epithelium in previous pathology studies (5). The most plausible explanation for reduced susceptibility of goblet cells to injury from 1-NN comes from previous studies of nasal epithelial cell ultra structure in rats. Harkema (36) reported that the NTE cells of rats are abundant in smooth endoplasmic reticulum (SER) and mitochondria but lack secretory granules. SER is particularly rich in xenobiotic-metabolizing enzymes such as P450; these enzymes are essential to the bioactivation and toxicity of 1-NN (2–4). In contrast, goblet cells are occupied mostly with rough endoplasmic reticulum (RER) in rat nasal tissues (J. R. Harkema, personal communication). As such, the observed reduction of 1-NN injury may be caused by replacement of NTE cells, a population with high xenobiotic-metabolizing capacity, with goblet cells, representing a cell population with limited capacity for *in situ* bioactivation of 1-NN. This theory also offers a credible explanation to the observed alterations in the protein adduct formation pattern caused by prior

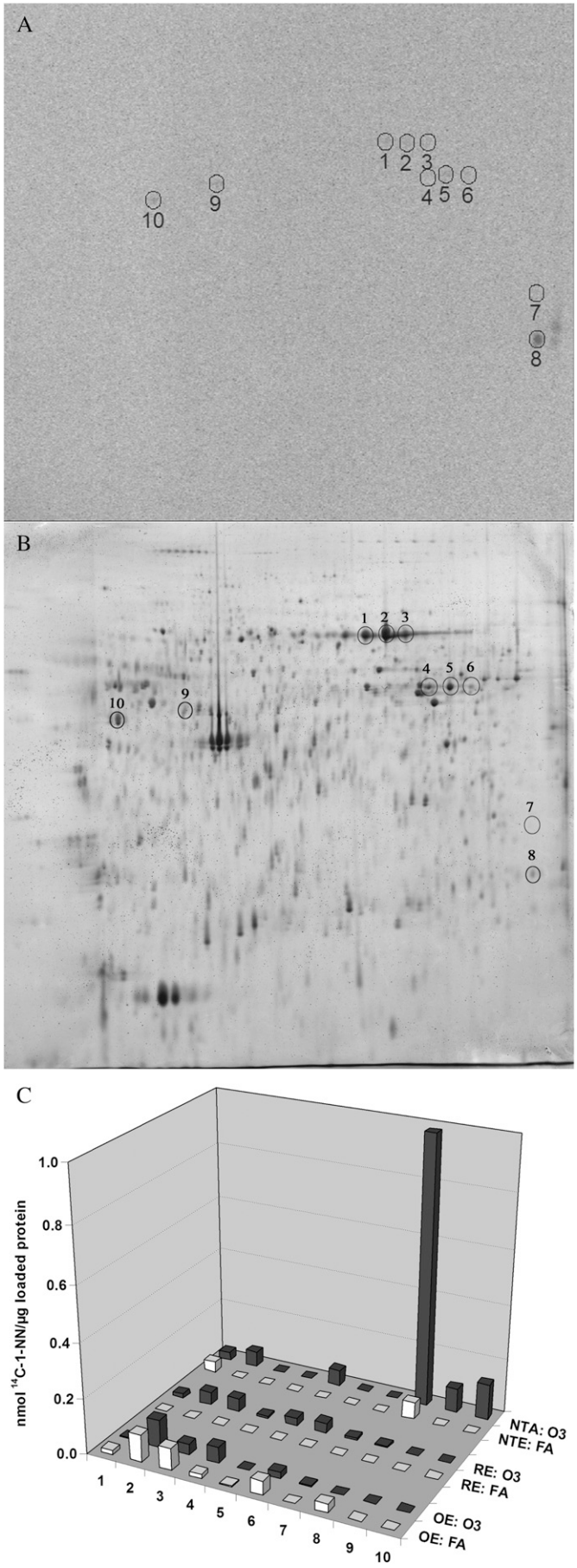

Figure 6. Adduction pattern of specific proteins by 1-NN metabolites in septal olfactory epithelium (OLF), septal nonolfactory epithelium (NON),and maxilloturbinate epithelium (MT) of FA-exposed versus ozone-exposed rats 2 hours post injection of 50 mg/kg ^{14}C-1-NN. *A* displays the storage phosphor image of NTE proteins from maxilloturbinate epithelium of ozone-exposed rat. *B* shows the location of the protein spots in the corresponding 2DE gel. *C* shows the relative adduction level (mol ^{14}C-1-NN/mol protein) for each of the individual protein spots in all analyzed tissues from ozone-exposed rat (*solid bars*) and FA-exposed control (*open bars*), respectively. The adduction of spot number 8 was drastically increased in NTE after ozone exposure, in spite of the overall decreased metabolite binding observed in this tissue.

ozone exposure, as the overall adduct formation was attenuated (Figure 5).

Reduced susceptibility to 1-NN–induced injury in goblet cells can also be attributed to mucins, which in goblet cells have been suggested to act as antioxidants by trapping reactive oxygen species in their oligosaccharide chains (18, 37). An important function of RER in goblet cells is mucin biosynthesis. Seventy to 80% of mucins are oligosaccharide chains by mass. Oligosaccharide chains on mucins modified by reactive oxygen species derived from ozone and/or 1-NN biotransformation may prevent other critical biomolecules from being functionally altered.

The major gel-forming mucins in both healthy and diseased lower airways of humans are MUC5AC and MUC5B (38). Immunohistochemical studies in nasal mucosa of nonallergic patients without inflammation have found that both MUC5AC and MUC5B show similar patterns of expression to lower airways (39). PAS-positive staining does not correlate with MUC5AC but with MUC5B in rabbits and humans (40, 41). Due to their lower density of negatively charged oligosaccharide chains as compared with AB-positive mucins, PAS-positive mucins are thought to contribute to a decrease in mucous hydration and a decrease in mucociliary clearance, which may cause pathologic conditions. Up-regulation of *MUC5B* gene products in the epithelium has been observed in a number of lower-airway diseases (asthma, chronic obstructive pulmonary disease, bronchiolitis) in mice and humans with inflammation and increased mucus production (42–44). In this study, mild inflammation that is indicated mostly by the presence of a low density of polymorphonuclear inflammatory cells in the underlying lamina propria of the nasal epithelium was the only sign of ozone-induced toxicity in nasal epithelium with goblet cell metaplasia. This ozone-induced, chronic lesion involves substantial up-regulation of PAS-positive mucosubstances in metaplastic goblet cells. It is possible that up-regulation of MUC5B has occurred via goblet cell metaplasia in ozone-tolerant rats. However, we were unable to examine the localization of MUC5B on the rat nasal sections due to the unavailability of specific antibodies to rat MUC5B. Cho and colleagues (21) have shown that in the nasal metaplastic epithelium of rats exposed to ozone (0.5 ppm, 8 h/d, 1 or 3 d), goblet cell metaplasia was neutrophil dependent. The *MUC5AC* gene transcript was up-regulated but occurred in a neutrophil-independent manner. Whether MUC5B is up-regulated in a neutrophil-dependent manner has not been examined.

The scenario of increased, mucin-mediated scavenging of electrophilic 1-NN metabolites also supports results from the reactive metabolite binding analyses. In spite of the overall down-regulation of adduction in NTE as a result of ozone exposure (Figure 5), the specific protein adduction appeared to be increased for three different protein spots (Figure 6, *spots 8–10*). Given that the prior ozone exposure showed a protective effect in histopathology, these three proteins may be acting as sinks for the

reactive 1-NN metabolites. CYP2B1 activity has been shown to be up-regulated 3-fold by prior long-term ozone exposure in airway epithelium (31). Although the corresponding level of induction has not been measured in nasal mucosa, an up-regulation of CYP2B1 in the few remaining NTE cells could explain maintained bioactivation and adduct formation to some extent, although decreased (Figure 5). In distal bronchioles, toxicity has been observed also in ciliated cells after high doses of 1-NN, although these cells lack the capability of activating the toxicant. It is plausible that the reactive 1-NN epoxides produced in the neighboring Clara cells are stable enough to cross the plasma membrane into the airway lumen or adjacent cells, and cause adduct formation also in non–CYP2B1-expressing cells. As such, the observed increased adduction of specific proteins (Figure 6, *spots 8–10*) in goblet cell metaplastic NTE could be derived from goblet cells. Given the protective effects seen in this epithelium, spots 8–10 are likely to be adducted at sites not essential to protein function, and thus act as sinks for the electrophilic 1-NN metabolites. Due to the low amounts of protein available in the NTE portion of the nasal mucosa, only low protein-load 2DE gels ($\sim 250\mu g$) with semi-broad ranges of isoelectric points (pH 4–7, 18 cm) could be analyzed, which hampered any attempts to identify the proteins by mass spectrometry (data not shown). Furthermore, the corresponding analysis of airway epithelium performed on the same rats (6) used ultra zoom 2DE, enabling a total load of 2 mg of protein and twice the spatial resolution for the same range. Consequently, the sensitivity of detection for the nasal analysis was very limited, and the proteins found to be of importance for the mechanism of toxicity of 1-NN, as well as the mechanism of ozone-induced synergism (Calreticulin, biliverdin reductase B, peroxiredoxin 6, and HSP B1 [6]) are likely to be below the detection limit in the current study. Further studies to outline CYP2B1 activity levels in specific cell types of the nasal epithelium as well as identification of adducted proteins need to be performed. Such studies would facilitate the elucidation of the mechanisms underlying the observed protective effects of ozone-induced goblet cell metaplasia on bioactivated toxicants such as 1-NN, and why the effects of ozone are opposing in the upper and lower respiratory epithelia.

In summary, rat nasal mucosa is injured by systemically administered 1-NN, with the worst lesions observed in NTE. NTE is also the main site of structural changes after long-term ozone exposure, and the resulting goblet cell metaplasia appears to confer protection of the nasal mucosa from 1-NN injury. Our findings suggest that goblet cells in rat nasal mucosa significantly protect nasal mucosa from acute injury by subsequent exposure to 1-NN, a toxicant that requires P450-mediated bioactivation. Potential mechanisms of the decreased susceptibility include decreased bioactivation of 1-NN as well as increased capacity of scavenging the reactive 1-NN metabolites due to increased mucin production.

Conflict of Interest Statement: None of the authors has a financial relationship with a commercial entity that has an interest in the subject of this manuscript.

Acknowledgments: The authors greatly appreciate Dr. Alan Buckpitt for providing rat nasal samples and for reading the manuscript critically. They also appreciate Dexter Morin for his generous help in animal treatment and necropsy and Dr. Michelle Fanucchi for fruitful discussions. The authors are grateful to Dr. Suzette Smiley-Jewell for help editing the manuscript, to Dr. Michael Evans for critical reading, to Dr. Brian Tarkington at the California Primate Center Exposure facility for assistance with ozone exposures, and to Dr. Lei Putney for lending us laboratory space during the necropsy.

References

1. Finlayson-Pitts BJ, Pitts JN Jr. Tropospheric air pollution: ozone, airborne toxics, polycyclic aromatic hydrocarbons, and particles. *Science* 1997;276:1045–1052.
2. Johnson DE, Riley MG, Cornish HH. Acute target organ toxicity of 1-nitronaphthalene in the rat. *J Appl Toxicol* 1984;4:253–257.
3. Halladay JS, Sauer JM, Sipes IG. Metabolism and disposition of [(14)c]1-nitronaphthalene in male sprague-dawley rats. *Drug Metab Dispos* 1999;27:1456–1465.
4. Shultz MA, Choudary PV, Buckpitt AR. Role of murine cytochrome p-450 2f2 in metabolic activation of naphthalene and metabolism of other xenobiotics. *J Pharmacol Exp Ther* 1999;290:281–288.
5. Paige RC, Wong V, Plopper CG. Long-term exposure to ozone increases acute pulmonary centriacinar injury by 1-nitronaphthalene: II. Quantitative histopathology. *J Pharmacol Exp Ther* 2000;295:942–950.
6. Wheelock AM, Boland BC, Isbell M, Morin D, Wegesser TC, Plopper CG, Buckpitt AR. In vivo effects of ozone exposure on protein adduct formation by 1-nitronaphthalene in rat lung. *Am J Respir Cell Mol Biol* 2005;33:130–137.
7. Buckpitt AR, Cruikshank MK. Biochemical function of the respiratory tract: metabolism of xenobiotics. In: Roth RA, editor. Comprehensive toxicology, vol 8: toxicology of the respiratory system, Oxford, UK: Elsevier Science Ltd.; 1997. pp. 159–186.
8. Harkema JR, Carey SA, Wagner JG. The nose revisited: a brief review of the comparative structure, function, and toxicologic pathology of the nasal epithelium. *Toxicol Pathol* 2006;34:252–269.
9. Thornton-Manning JR, Dahl AR. Metabolic capacity of nasal tissue interspecies comparisons of xenobiotic-metabolizing enzymes. *Mutat Res* 1997;380:43–59.
10. Gervasi PG, Longo V, Naldi F, Panattoni G, Ursino F. Xenobiotic-metabolizing enzymes in human respiratory nasal mucosa. *Biochem Pharmacol* 1991;41:177–184.
11. Longo V, Pacifici GM, Panattoni G, Ursino F, Gervasi PG. Metabolism of diethylnitrosamine by microsomes of human respiratory nasal mucosa and liver. *Biochem Pharmacol* 1989;38:1867–1869.
12. Su T, Bao Z, Zhang QY, Smith TJ, Hong JY, Ding X. Human cytochrome p450 cyp2a13: Predominant expression in the respiratory tract and its high efficiency metabolic activation of a tobacco-specific carcinogen, 4-(methylnitrosamino)-1-(3-pyridyl)-1-butanone. *Cancer Res* 2000;60:5074–5079.
13. Gu J, Su T, Chen Y, Zhang QY, Ding X. Expression of biotransformation enzymes in human fetal olfactory mucosa: potential roles in developmental toxicity. *Toxicol Appl Pharmacol* 2000;165:158–162.
14. Chen Y, Liu YQ, Su T, Ren X, Shi L, Liu D, Gu J, Zhang QY, Ding X. Immunoblot analysis and immunohistochemical characterization of cyp2a expression in human olfactory mucosa. *Biochem Pharmacol* 2003; 66:1245–1251.
15. Foy JW, Schatz RA. Inhibition of rat respiratory-tract cytochrome p-450 activity after acute low-level m-xylene inhalation: role in 1-nitronaphthalene toxicity. *Inhal Toxicol* 2004;16:125–132.
16. Verschoyle RD, Carthew P, Wolf CR, Dinsdale D. 1-nitronaphthalene toxicity in rat lung and liver: effects of inhibiting and inducing cytochrome p450 activity. *Toxicol Appl Pharmacol* 1993;122:208–213.
17. Cho HY, Hotchkiss JA, Harkema JR. Inflammatory and epithelial responses during the development of ozone-induced mucous cell metaplasia in the nasal epithelium of rats. *Toxicol Sci* 1999;51:135–145.
18. Harkema JR, Hotchkiss JA, Griffith WC. Mucous cell metaplasia in rat nasal epithelium after a 20-month exposure to ozone: a morphometric study of epithelial differentiation. *Am J Respir Cell Mol Biol* 1997;16: 521–530.
19. Harkema JR, Plopper CG, Hyde DM, St George JA, Dungworth DL. Effects of an ambient level of ozone on primate nasal epithelial mucosubstances: quantitative histochemistry. *Am J Pathol* 1987;127: 90–96.
20. Harkema JR, Plopper CG, Hyde DM, St George JA, Wilson DW, Dungworth DL. Response of the macaque nasal epithelium to ambient levels of ozone: a morphologic and morphometric study of the transitional and respiratory epithelium. *Am J Pathol* 1987;128:29–44.
21. Cho HY, Hotchkiss JA, Bennett CB, Harkema JR. Neutrophil-dependent and neutrophil-independent alterations in the nasal epithelium of ozone-exposed rats. *Am J Respir Crit Care Med* 2000;162:629–636.
22. Koren HS, Hatch GE, Graham DE. Nasal lavage as a tool in assessing acute inflammation in response to inhaled pollutants. *Toxicology* 1990; 60:15–25.
23. Gerrity TR, Weaver RA, Berntsen J, House DE, O'Neil JJ. Extrathoracic and intrathoracic removal of o3 in tidal-breathing humans. *J Appl Physiol* 1988;65:393–400.
24. Barr BC, Hyde DM, Plopper CG, Dungworth DL. A comparison of terminal airway remodeling in chronic daily versus episodic ozone exposure. *Toxicol Appl Pharmacol* 1990;106:384–407.
25. Young JT. Histopathologic examination of the rat nasal cavity. *Fundam Appl Toxicol* 1981;1:309–312.

26. Hyde DM, Plopper CG, George JA, Harkema JR. Morphometric cell biology of air space epithelium. In: Schraufnagel D, editor. Electron microscopy of the lung. New York: Dekker; 1990. pp. 71–120.
27. Bradford MM. A rapid and sensitive method for the quantitation of microgram quantities of protein utilizing the principle of protein-dye binding. *Anal Biochem* 1976;72:248–254.
28. Van Winkle LS, Johnson ZA, Nishio SJ, Brown CD, Plopper CG. Early events in naphthalene-induced acute clara cell toxicity: comparison of membrane permeability and ultrastructure. *Am J Respir Cell Mol Biol* 1999;21:44–53.
29. Plopper CG, Van Winkle LS, Fanucchi MV, Malburg SR, Nishio SJ, Chang A, Buckpitt AR. Early events in naphthalene-induced acute clara cell toxicity: II. Comparison of glutathione depletion and histopathology by airway location. *Am J Respir Cell Mol Biol* 2001;24:272–281.
30. Paige R, Wong V, Plopper C. Dose-related airway-selective epithelial toxicity of 1-nitronaphthalene in rats. *Toxicol Appl Pharmacol* 1997; 147:224–233.
31. Paige RC, Royce FH, Plopper CG, Buckpitt AR. Long-term exposure to ozone increases acute pulmonary centriacinar injury by 1-nitronaphthalene: I. Region-specific enzyme activity. *J Pharmacol Exp Ther* 2000; 295:934–941.
32. Lee MG, Phimister A, Morin D, Buckpitt A, Plopper C. In situ naphthalene bioactivation and nasal airflow cause region-specific injury patterns in the nasal mucosa of rats exposed to naphthalene by inhalation. *J Pharmacol Exp Ther* 2005;314:103–110.
33. West JA, Pakehham G, Morin D, Fleschner CA, Buckpitt AR, Plopper CG. Inhaled naphthalene causes dose dependent clara cell cytotoxicity in mice but not in rats. *Toxicol Appl Pharmacol* 2001;173:114–119.
34. Warren DL, Brown DL Jr, Buckpitt AR. Evidence for cytochrome p-450 mediated metabolism in the bronchiolar damage by naphthalene. *Chem Biol Interact* 1982;40:287–303.
35. Verschoyle RD, Dinsdale D. Protection against chemical-induced lung injury by inhibition of pulmonary cytochrome p-450. *Environ Health Perspect* 1990;85:95–100.
36. Harkema JR. Epithelial cells in the nasal passages. In: Parent R, editor. Comparative biology of the normal lung. Boca Raton: CRC Press; 1992. pp. 27–36.
37. Cross CE, Halliwell B, Allen A. Antioxidant protection: a function of tracheobronchial and gastrointestinal mucus. *Lancet* 1984;1:1328–1330.
38. Davies JR, Svitacheva N, Lannefors L, Kornfalt R, Carlstedt I. Identification of muc5b, muc5ac and small amounts of muc2 mucins in cystic fibrosis airway secretions. *Biochem J* 1999;344:321–330.
39. Groneberg DA, Peiser C, Dinh QT, Matthias J, Eynott PR, Heppt W, Carlstedt I, Witt C, Fischer A, Chung KF. Distribution of respiratory mucin proteins in human nasal mucosa. *Laryngoscope* 2003;113: 520–524.
40. Sheehan JK, Howard M, Richardson PS, Longwill T, Thornton DJ. Physical characterization of a low-charge glycoform of the muc5b mucin comprising the gel-phase of an asthmatic respiratory mucous plug. *Biochem J* 1999;338:507–513.
41. Schousboe LP, Rasmussen LM, Ovesen T. Induction of mucin and adhesion molecules in middle ear mucosa. *Acta Otolaryngol* 2001;121:596–601.
42. Chen Y, Zhao YH, Wu R. In silico cloning of mouse muc5b gene and upregulation of its expression in mouse asthma model. *Am J Respir Crit Care Med* 2001;164:1059–1066.
43. Caramori G, Di Gregorio C, Carlstedt I, Casolari P, Guzzinati I, Adcock IM, Barnes PJ, Ciaccia A, Cavallesco G, Chung KF, *et al.* Mucin expression in peripheral airways of patients with chronic obstructive pulmonary disease. *Histopathology* 2004;45:477–484.
44. Kamio K, Matsushita I, Hijikata M, Kobashi Y, Tanaka G, Nakata K, Ishida T, Tokunaga K, Taguchi Y, Homma S, *et al.* Promoter analysis and aberrant expression of the muc5b gene in diffuse panbronchiolitis. *Am J Respir Crit Care Med* 2005;171:949–957.
45. Schmelzer KR, Wheelock AM, Dettmer K, Morin D, Hammock BD. The role of inflammatory mediators in the synergistic toxicity of ozone and 1-nitronaphthalene in rat airways. *Environ Health Perspect* 2006;114:1354–1360.